4578 *Inorg. Chem.* **2010**, *49*, 4578–4585
DOI: 10.1021/ic100292u

Inorganic Chemistry
Article

Synthesis, Characterization, and Structures of Divalent Europium and Ytterbium *N,N*-Dimethylaminodiboranates

Scott R. Daly and Gregory S. Girolami*

The School of Chemical Sciences, University of Illinois at Urbana−Champaign, 600 South Mathews Avenue, Urbana, Illinois 61801

Received February 11, 2010

Treatment of the trichlorides $EuCl_3$ and $YbCl_3$ with $Na(H_3BNMe_2BH_3)$ in tetrahydrofuran (THF) results in a reduction to the corresponding divalent europium and ytterbium *N,N*-dimethylaminodiboranate (DMADB) complexes $Eu(H_3BNMe_2BH_3)_2(THF)_2$ (**1**) and $Yb(H_3BNMe_2BH_3)_2(THF)_2$ (**2**), which can be separated from trivalent $Ln(H_3BNMe_2BH_3)_3(THF)$ byproducts by extraction and crystallization from pentane. No other lanthanide trihalides react with $Na(H_3BNMe_2BH_3)$ to afford divalent products. Compounds **1** and **2** can also be prepared from the divalent lanthanide iodides EuI_2 and YbI_2 in higher yield and without the need to separate them from trivalent species. Treatment of **1** and **2** with an excess of 1,2-dimethoxyethane (DME) in pentane affords the new species $Eu(H_3BNMe_2BH_3)_2(DME)_2$ (**3**) and $Yb(H_3BNMe_2BH_3)_2(DME)$ (**4**). Compound **1** is dinuclear: each metal center is bound to two chelating DMADB ligands, one of which also bridges to the other metal. Overall, the coordination geometry about each Eu atom can be described as a distorted pentagonal bipyramid, with five B atoms from the DMADB ligands occupying the equatorial sites and two THF molecules occupying the axial sites. Unlike **1**, compound **2** is monomeric owing to the smaller radius of Yb^{II} versus Eu^{II}; the B and O atoms describe a distorted cis octahedron. The Eu(DME) complex **3** is also monomeric; both DMADB ligands and both DME molecules chelate to the metal center. The four B atoms and the four O atoms describe a distorted square antiprism, with the O atoms occupying one square face and the B atoms occupying the other. In addition to X-ray crystallographic studies, IR, NMR, and mass spectrometric data are reported for all four new compounds.

Introduction

Although the 3+ oxidation state dominates the solution chemistry of the lanthanide elements, it has been known since 1906 that some of the lanthanides also have accessible divalent oxidation states.[1] In recent years, there has been a remarkable expansion in the availability of lanthanide dihalide starting materials;[2−6] as a result, divalent complexes are now known for many of the lanthanides.[7−11] In addition, divalent species such as SmI_2 find use in organic syntheses as powerful one-electron reductants; for example, they are widely used to promote the coupling of alkyl halides with ketones to form tertiary alcohols.[12−18]

The 2+ oxidation state of lanthanides can be accessed either by oxidation of the bulk metal or by reduction of trivalent lanthanide species. The reduction of Ln^{3+} to Ln^{2+} can be accomplished by comproportionation reactions involving Ln^0 metal; alternatively, such reductions can be achieved by the addition of an alkali metal.[19,20] There are also a few examples in which the reduction of Ln^{3+} to Ln^{2+} is effected by a reagent that serves both as a reductant and as a

*To whom correspondence should be addressed. E-mail: ggirolam@uiuc.edu.

(1) Matignon, C.; Cazes, E. *C. R.* **1906**, *142*, 83–85.
(2) Girard, P.; Namy, J. L.; Kagan, H. B. *J. Am. Chem. Soc.* **1980**, *102*, 2693–2698.
(3) Bochkarev, M. N.; Fedushkin, I. L.; Fagin, A. A.; Petrovskaya, T. V.; Ziller, J. W.; Broomhall-Dillard, R. N. R.; Evans, W. J. *Angew. Chem., Int. Ed.* **1997**, *36*, 133–135.
(4) Evans, W. J.; Allen, N. T.; Ziller, J. W. *J. Am. Chem. Soc.* **2000**, *122*, 11749–11750.
(5) Bochkarev, M. N.; Fedushkin, I. L.; Dechert, S.; Fagin, A. A.; Schumann, H. *Angew. Chem., Int. Ed.* **2001**, *40*, 3176–3178.
(6) Evans, W. J.; Allen, N. T.; Workman, P. S.; Meyer, J. C. *Inorg. Chem.* **2003**, *42*, 3097–3099.
(7) Bochkarev, M. N. *Coord. Chem. Rev.* **2004**, *248*, 835–851.
(8) Hitchcock, P. B.; Lappert, M. F.; Maron, L.; Protchenko, A. V. *Angew. Chem., Int. Ed.* **2008**, *47*, 1488–1491.
(9) Evans, W. J. *J. Organomet. Chem.* **2002**, *647*, 2–11.
(10) Evans, W. J. *Inorg. Chem.* **2007**, *46*, 3435–3449.
(11) Evans, W. J. *J. Alloys Compd.* **2009**, *488*, 493–510.
(12) Kagan, H. B.; Namy, J.-L. *Top. Organomet. Chem.* **1999**, *2*, 155–198.
(13) Krief, A.; Laval, A.-M. *Chem. Rev.* **1999**, *99*, 745–777.
(14) Mikami, K.; Terada, M.; Matsuzawa, H. *Angew. Chem., Int. Ed.* **2002**, *41*, 3554–3571.
(15) Kagan, H. B. *Tetrahedron* **2003**, *59*, 10351–10372.
(16) Berndt, M.; Gross, S.; Hoelemann, A.; Reissig, H.-U. *Synlett* **2004**, 422–438.
(17) Dahlen, A.; Hilmersson, G. *Eur. J. Inorg. Chem.* **2004**, 3393–3403.
(18) Edmonds, D. J.; Johnston, D.; Procter, D. *J. Chem. Rev.* **2004**, *104*, 3371–3403.
(19) Corbett, J. D. In *Topics in f-Element Chemistry*; Meyer, G., Morss, L. R., Eds.; Kluwer Academic: Dordrecht, The Netherlands, 1991; Vol. *2*, pp 159−173.

 Published on Web 04/14/2010

ligand for the metal center; this approach invariably involves the most easily reduced lanthanides Eu, Yb, and Sm.[21] For example, reactions of europium(III) halides with bulky cyclopentadienide anions or of europium(III) metallocene halides with alkyllithium reagents can afford organometallic compounds of Eu^{II}.[22−25] The Yb^{III} complex $[(C_5H_4Me)_2YbMe]_2$ slowly reduces to the corresponding $(C_5H_4Me)_2Yb$ complex upon being heated to 80 °C or photolyzed in toluene.[26] The reactions of $Ln[N(SiMe_3)_2]_3(\mu\text{-}Cl)Li(THF)_3$, where Ln = Eu or Yb, with indenes or fluorenes bearing pendant amine or ether functional groups, yield the corresponding lanthanide(II) metallocenes.[27−37] Similarly, treatment of the substituted benzyl complex $Sm(CH_2C_6H_4\text{-}2\text{-}NMe_2)_3$ with the bulky cyclopentadiene $C_5(C_6H_4\text{-}4\text{-}n\text{-}Bu)_5H$ ($Cp^{BIG}H$) at 60 °C yields the Sm^{II} product $Sm(Cp^{BIG})_2$.[38]

A closely related phenomenon is sterically induced reduction,[9−11,39,40] which is characteristic of tris(pentamethylcyclopentadienyl) complexes $Ln(C_5Me_5)_3$. The C_5Me_5 ligand is not usually redox-active, but the $Ln(C_5Me_5)_3$ complexes are sufficiently crowded that there is a strong driving force to eliminate one of the rings. As a result, these complexes react with various substrates to give products that appear to have been generated via the divalent intermediate $Ln(C_5Me_5)_2$.[41−45]

All of the above reactions involve organic ligands, but there are other chemical groups that can also serve both as a reductant and as a ligand. Prominent among these is tetrahydroborate, BH_4^-, a ligand known for its reducing power.[46,47] For example, treatment of most lanthanide trichlorides with BH_4^- in THF at room temperature affords trivalent borohydride complexes, but $EuCl_3$ is reduced to Eu^{II}.[48] The Ln^{II} complexes $Ln(BH_4)_2(THF)_2$, where Ln = Eu, Yb, and Sm, have been prepared by decomposing $NaLn(BH_4)_4(DME)_4$ at 150−200 °C under a dynamic vacuum.[49]

Most divalent lanthanide borohydride complexes, however, are synthesized from divalent starting materials. For example, the pyridine and acetonitrile complexes $Ln(BH_4)_2(py)_4$ and $Ln(BH_4)_2(MeCN)_4$ have been prepared by treating $EuCl_2$ and $YbCl_2$ with $NaBH_4$.[50] Similar reactions afford Eu^{II} and Yb^{II} complexes of the organohydroborate $H_2BC_8H_{14}^-$ (9-BBN)[51,52] In addition, the heteroleptic ytterbium pyrazolylborate $(Tp^{tBu,Me})Yb(BH_4)$ has been prepared by metathesis from $(Tp^{tBu,Me})YbI(THF)$ and also by the addition of $BH_3\cdot NMe_3$ to the ytterbium hydride $[(Tb^{tBu,Me})YbH]_2$.[53] Finally, one divalent lanthanide tetrahydroborate has been prepared by oxidation of the metal: the reaction of ytterbium amalgam with $BH_3\cdot THF$ affords a mixture of $Yb(BH_4)_2$ and $Yb(B_3H_8)_2$.[54]

We have recently been exploring the chemistry of a new class of multidentate borohydride ligands known as the aminodiboranates.[55−58] We have previously shown that *N*,*N*-dimethylaminodiboranate (DMADB) complexes of trivalent lanthanide are highly volatile and useful as chemical vapor deposition and atomic layer deposition precursors to lanthanide-containing thin films.[59] We now describe the synthesis, characterization, and molecular structures of divalent lanthanide *N*,*N*-dimethylaminodiboranates. In several of these reactions, the DMADB ligand serves simultaneously as a ligand and as a reductant.

Results and Discussion

Synthesis of $Ln(H_3BNMe_2BH_3)_2(THF)_2$ and $Ln(H_3BNMe_2BH_3)_2(DME)_x$, where Ln = Eu and Yb. Treatment of the trichlorides $EuCl_3$ or $YbCl_3$ with $Na(H_3BNMe_2BH_3)$ in THF results in a reduction to the corresponding divalent europium and ytterbium *N*,*N*-dimethylaminodiboranate complexes $Eu(H_3BNMe_2BH_3)_2(THF)_2$ (**1**) and $Yb(H_3BNMe_2BH_3)_2(THF)_2$ (**2**). The products can be isolated

(20) Meyer, G.; Schleid, T. In *Topics in f-Element Chemistry*; Meyer, G., Morss, L. R., Eds.; Kluwer Academic: Dordrecht, The Netherlands, 1991; Vol. *2*, pp 175−185.
(21) Morss, L. R. *Chem. Rev.* **1976**, *76*, 827–842.
(22) Tilley, T. D.; Andersen, R. A.; Spencer, B.; Ruben, H.; Zalkin, A.; Templeton, D. H. *Inorg. Chem.* **1980**, *19*, 2999–3003.
(23) Arnaudet, L.; Ban, B. *New J. Chem.* **1988**, *12*, 201–203.
(24) Sitzmann, H.; Dezember, T.; Schmitt, O.; Weber, F.; Wolmershauser, G.; Ruck, M. *Z. Anorg. Allg. Chem.* **2000**, *626*, 2241–2244.
(25) Gudilenkov, I. D.; Fukin, G. K.; Baranov, E. V.; Trifonov, A. A. *Russ. Chem. Bull.* **2008**, *57*, 40–46.
(26) Zinnen, H. A.; Pluth, J. J.; Evans, W. J. *J. Chem. Soc., Chem. Commun.* **1980**, 810–812.
(27) Sheng, E.; Wang, S.; Yang, G.; Zhou, S.; Cheng, L.; Zhang, K.; Huang, Z. *Organometallics* **2003**, *22*, 684–692.
(28) Zhang, K.; Zhang, W.; Wang, S.; Sheng, E.; Yang, G.; Xie, M.; Zhou, S.; Feng, Y.; Mao, L.; Huang, Z. *Dalton Trans.* **2004**, 1029–1037.
(29) Sheng, E.; Zhou, S.; Wang, S.; Yang, G.; Wu, Y.; Feng, Y.; Mao, L.; Huang, Z. *Eur. J. Inorg. Chem.* **2004**, 2923–2932.
(30) Wu, Y.; Wang, S.; Qian, C.; Sheng, E.; Xie, M.; Yang, G.; Feng, Q.; Zhang, L.; Tang, X. *J. Organomet. Chem.* **2005**, *690*, 4139–4149.
(31) Wang, S.; Feng, Y.; Mao, L.; Sheng, E.; Yang, G.; Xie, M.; Wang, S.; Wei, Y.; Huang, Z. *J. Organomet. Chem.* **2006**, *691*, 1265–1274.
(32) Wang, S.; Tang, X.; Vega, A.; Saillard, J.-Y.; Sheng, E.; Yang, G.; Zhou, S.; Huang, Z. *Organometallics* **2006**, *25*, 2399–2401.
(33) Wang, S.; Wang, S.; Zhou, S.; Yang, G.; Luo, W.; Hu, N.; Zhou, Z.; Song, H. *J. Organomet. Chem.* **2007**, *692*, 2099–2106.
(34) Zhou, S.; Wang, S.; Sheng, E.; Zhang, L.; Yu, Z.; Xi, X.; Chen, G.; Luo, W.; Li, Y. *Eur. J. Inorg. Chem.* **2007**, 1519–1528.
(35) Cheng, L.; Feng, Y.; Wang, S.; Luo, W.; Yao, W.; Yu, Z.; Xi, X.; Huang, Z. *Eur. J. Inorg. Chem.* **2007**, 1770–1777.
(36) Wang, S.; Tang, X.; Vega, A.; Saillard, J.-Y.; Zhou, S.; Yang, G.; Yao, W.; Wei, Y. *Organometallics* **2007**, *26*, 1512–1522.
(37) Wei, Y.; Yu, Z.; Wang, S.; Zhou, S.; Yang, G.; Zhang, L.; Chen, G.; Qian, H.; Fan, J. *J. Organomet. Chem.* **2008**, *693*, 2263–2270.
(38) Ruspic, C.; Moss, J. R.; Schuermann, M.; Harder, S. *Angew. Chem., Int. Ed.* **2008**, *47*, 2121–2126.
(39) Evans, W. J.; Davis, B. L. *Chem. Rev.* **2002**, *102*, 2119–2136.
(40) Evans, W. J. *Coord. Chem. Rev.* **2000**, *206*−*207*, 263–283.
(41) Evans, W. J.; Forrestal, K. J.; Ziller, J. W. *J. Am. Chem. Soc.* **1995**, *117*, 12635–12636.
(42) Evans, W. J.; Forrestal, K. J.; Ziller, J. W. *J. Am. Chem. Soc.* **1998**, *120*, 9273–9282.
(43) Evans, W. J.; Nyce, G. W.; Clark, R. D.; Doedens, R. J.; Ziller, J. W. *Angew. Chem., Int. Ed.* **1999**, *38*, 1801–1803.
(44) Evans, W. J.; Perotti, J. M.; Kozimor, S. A.; Champagne, T. M.; Davis, B. L.; Nyce, G. W.; Fujimoto, C. H.; Clark, R. D.; Johnston, M. A.; Ziller, J. W. *Organometallics* **2005**, *24*, 3916–3931.
(45) Evans, W. J.; Davis, B. L.; Champagne, T. M.; Ziller, J. W. *Proc. Natl. Acad. Sci. U.S.A.* **2006**, *103*, 12678–12683.
(46) Marks, T. J.; Kolb, J. R. *Chem. Rev.* **1977**, *77*, 263–293.
(47) Pelter, A.; Smith, K.; Brown, H. C. *Borane Reagents*; Academic Press: San Diego, 1988; p 503.
(48) Rossmanith, K.; Muckenhuber, E. *Monatsh. Chem.* **1961**, *92*, 600–604.
(49) Makhaev, V. D.; Borisov, A. P. *Russ. J. Inorg. Chem.* **1999**, *44*, 1411–1413.
(50) White, J. P., III; Deng, H.; Shore, S. G. *Inorg. Chem.* **1991**, *30*, 2337–2342.
(51) Chen, X.; Lim, S.; Plecnik, C. E.; Liu, S.; Du, B.; Meyers, E. A.; Shore, S. G. *Inorg. Chem.* **2004**, *43*, 692–698.
(52) Chen, X.; Lim, S.; Plecnik, C. E.; Liu, S.; Du, B.; Meyers, E. A.; Shore, S. G. *Inorg. Chem.* **2005**, *44*, 6052–6061.
(53) Saliu, K. O.; Maunder, G. H.; Ferguson, M. J.; Sella, A.; Takats, J. *Inorg. Chim. Acta* **2009**, *362*, 4616–4622.
(54) Hill, T. G.; Godfroid, R. A.; White, J. P., III; Shore, S. G. *Inorg. Chem.* **1991**, *30*, 2952–2954.
(55) Keller, P. C. *J. Chem. Soc. D* **1969**, 1465.
(56) Keller, P. C. *Inorg. Chem.* **1971**, *10*, 2256–2259.
(57) Nöth, H.; Thomas, S. *Eur. J. Inorg. Chem.* **1999**, 1373–1379.
(58) Daly, S. R.; Girolami, G. S. *Chem. Commun.* **2010**, *46*, 407–408.
(59) Daly, S. R.; Kim, D. Y.; Yang, Y.; Abelson, J. R.; Girolami, G. S. *J. Am. Chem. Soc.* **2010**, *132*, 2106–2107.

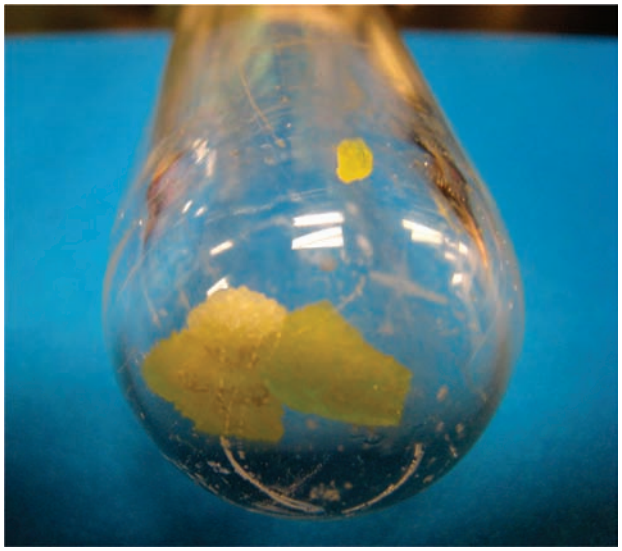

Figure 1. Second crystallization crop from the reaction of $EuCl_3$ and $Na(H_3BNMe_2BH_3)$ at −78 °C. Both off-white **1** and yellow $Eu(H_3BNMe_2BH_3)_3(THF)$ are present.

from their reaction residues by extraction and crystallization from pentane:

$$LnCl_3 + 3Na(H_3BNMe_2BH_3) \xrightarrow{THF}$$
$$Ln(H_3BNMe_2BH_3)_2(THF)_2 + \frac{1}{2}H_2 + (NMe_2)B_2H_5 + 3NaCl$$
$$Ln = Eu\ (\mathbf{1}),\ Yb\ (\mathbf{2})$$

The reactions of $EuCl_3$ and $YbCl_3$ with $Na(H_3BNMe_2BH_3)$ are not quantitative, but instead both produce a mixture of these divalent products and the corresponding trivalent species $Ln(H_3BNMe_2BH_3)_3(THF)$, which we have described elsewhere.[59] The divalent and trivalent products can be easily distinguished by their colors. The Eu^{2+} complex **1** is off-white, whereas its Eu^{3+} analogue is yellow; for ytterbium, the colors are reversed: the Yb^{2+} complex **2** is intensely yellow, whereas the Yb^{3+} analogue is pale-yellow. We have been unable to obtain Sm^{2+} products from similar reactions starting from $SmCl_3$.

The relative amounts of Ln^{2+} and Ln^{3+} products isolated from the reactions of $YbCl_3$ and $EuCl_3$ with $Na(H_3BNMe_2BH_3)$ appear to depend on the reaction temperature. Specifically, the addition of $Na(H_3BNMe_2BH_3)$ to $EuCl_3$ at −78 °C yields the Eu^{III} complex as the major product, whereas the same addition carried out at 0 °C largely yields the Eu^{II} complex. A similar trend is seen for Yb: at 0 °C, more of the Yb^{III} complex is isolated, whereas at 25 °C, the Yb^{II} complex is the major product. Generally, the first crop of crystals obtained from pentane generally consists of pure material (either Ln^{2+} or Ln^{3+} depending on the reaction conditions used); subsequent crops are increasingly enriched with the minor species (Figure 1).

The formation of a mixture of products can be avoided by employing the divalent lanthanide iodides EuI_2 and YbI_2 as starting materials. Treatment of these salts with $Na(H_3BNMe_2BH_3)$ affords **1** and **2** in 53−74% yield;

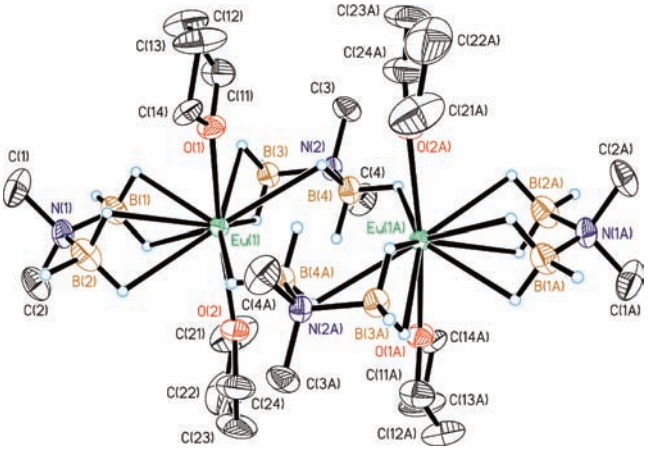

Figure 2. Molecular structure of **1**. Ellipsoids are drawn at the 35% probability level. H atoms attached to C atoms and disordered components have been deleted for clarity.

analogous reactions using the divalent chlorides $LnCl_2$ are unsuccessful.

$$LnI_2 + 2Na(H_3BNMe_2BH_3) \xrightarrow{THF}$$
$$Ln(H_3BNMe_2BH_3)_2(THF)_2 + 2NaI$$
$$Ln = Eu\ (\mathbf{1}),\ Yb\ (\mathbf{2})$$

The THF molecules in **1** and **2** can be readily displaced by treatment with an excess of 1,2-dimethoxyethane (DME) in pentane to afford the new species $Eu(H_3BNMe_2BH_3)_2(DME)_2$ (**3**) and $Yb(H_3BNMe_2BH_3)_2(DME)$ (**4**). The different numbers of coordinated DME molecules in the two compounds are consistent with the larger size of Eu^{II} versus Yb^{II} (see below).

$$Ln(H_3BNMe_2BH_3)_2(THF)_2 + \text{xs DME} \xrightarrow{\text{pentane}}$$
$$Ln(H_3BNMe_2BH_3)_2(DME)_x + 2THF$$
$$Ln = Eu\ (\mathbf{3},\ x = 2),\ Yb\ (\mathbf{4},\ x = 1)$$

The divalent lanthanide DMADB complexes do not show any appreciable volatility except for **4**, which upon heating to 65−75 °C at 10^{-2} Torr gives a low (10%) yield of a sublimate. The recovered sublimate is not soluble in toluene (whereas **4** is quite soluble in this solvent). These results suggest that **1**−**4** desolvate when heated under vacuum.

Crystal Structures. Although the THF adducts **1** and **2** have the same stoichiometry, they have different solid-state structures. The Eu compound **1** is dinuclear: each metal center is bound to two chelating DMADB ligands, one of which also bridges to the other metal (Figure 2). Overall, the coordination geometry about each Eu atom can be described as a distorted pentagonal bipyramid, in which five B atoms from the DMADB ligands occupy the equatorial sites and two THF molecules occupy the axial sites. The B−Eu−O angles are all close to 90°, ranging from 82.5(1)° to 96.2(1)°, and the O1−Eu1−O2 angle deviates slightly from linearity at 167.91(6)° (Table 2).

The Eu···B distances to the non-bridging B atoms B1, B2, and B3 are 2.885(4), 3.127(4), and 2.991(4) Å, respectively. These distances are slightly longer than those of

Table 1. Crystallographic Data for **1**−**3** at 193 K

	1	**2**	**3**
formula	$C_{24}H_{80}B_8N_4O_4Eu_2$	$C_{12}H_{40}B_4N_2O_2Yb$	$C_{12}H_{44}B_4N_2O_4Eu$
fw (g mol^{-1})	879.32	460.74	475.69
λ (Å)	0.710 73	0.710 73	0.710 73
cryst syst	monoclinic	monoclinic	monoclinic
space group	$P2_1/c$	$P2_1/n$	$P2_1/n$
a (Å)	10.2155(2)	9.3382(10)	10.4304(11)
b (Å)	20.5596(5)	21.0643(3)	14.3523(15)
c (Å)	10.4732(3)	11.3500(13)	16.6107(18)
β (deg)	90.5740(10)	94.452(2)	103.552(6)
V (Å^3)	2199.54(9)	2225.8(4)	2417.4(4)
Z	2	4	4
ρ_{calc} (g cm^{-3})	1.328	1.375	1.307
μ (mm^{-1})	2.854	4.204	2.608
R(int)	0.0723	0.1040	0.0869
abs corrn	face-indexed	face-indexed	face-indexed
max, min transm factors	0.734, 0.594	0.166, 0.028	0.792, 0.544
data/restraints/param	4865/34/306	5780/68/242	5347/34/264
GOF on F^2	0.999	1.005	0.961
$R1$ [$I > 2\sigma(I)$][a]	0.0285	0.0377	0.0227
$wR2$ (all data)[b]	0.0766	0.1036	0.0548

[a] $R1 = \sum||F_o| - |F_c||/\sum|F_o|$ for reflections with $F_o^2 > 2\sigma(F_o^2)$. [b] $wR2 = [\sum w(F_o^2 - F_c^2)^2/\sum(F_o^2)^2]^{1/2}$ for all reflections.

Table 2. Selected Bond Lengths and Angles for **1**[a]

Bond Lengths (Å)			
Eu(1)−O(1)	2.5820(19)	Eu(1)−B(3)	2.991(4)
Eu(1)−O(2)	2.605(2)	Eu(1)−B(4)	3.215(6)
Eu(1)−B(1)	2.885(4)	Eu(1)−B(4)′	2.975(4)
Eu(1)−B(2)	3.127(4)	Eu(1)−Eu(1)′	4.741(4)
Bond Angles (deg)			
O(1)−Eu(1)−O(2)	167.91(6)	B(1)−Eu(1)−B(3)	82.86(10)
O(1)−Eu(1)−B(1)	96.13(10)	B(1)−Eu(1)−B(4)	132.05(10)
O(1)−Eu(1)−B(2)	87.36(9)	B(1)−Eu(1)−B(4)′	147.84(13)
O(1)−Eu(1)−B(3)	96.23(11)	B(3)−Eu(1)−B(2)	133.91(10)
O(1)−Eu(1)−B(4)	86.95(12)	B(2)−Eu(1)−B(4)	173.81(13)
O(1)−Eu(1)−B(4)′	85.42(13)	B(2)−Eu(1)−B(4)′	97.04(13)
O(2)−Eu(1)−B(1)	93.53(10)	B(3)−Eu(1)−B(4)	49.33(11)
O(2)−Eu(1)−B(2)	93.09(10)	B(3)−Eu(1)−B(4)′	129.03(14)
O(2)−Eu(1)−B(3)	92.16(11)	B(4)−Eu(1)−B(4)′	80.09(13)
O(2)−Eu(1)−B(4)	91.97(12)	B(2)−N(1)−B(1)	110.9(2)
O(2)−Eu(1)−B(4)′	82.53(13)	B(3)−N(2)−B(4)	111.6(4)
B(1)−Eu(1)−B(2)	51.13(9)		

[a] Symmetry transformation used to generate equivalent atoms: $-x+1$, $-y+1$, $-z$.

2.794(6)−2.920(7) Å observed for the κ^2H borohydride groups in $Eu(H_2BC_8H_{14})_2(THF)_4$ and similar complexes.[51,52] The H atom locations in **1** show that two H atoms bridge the Eu···B1 and Eu···B3 contacts, with Eu−H hydrogen distances of 2.44−2.68 Å (the H atom locations were refined but idealized; the errors in these distances are on the order of 0.05 Å). The longer Eu···B2 contact is also best thought of as involving a κ^2H interaction, although one of the Eu−H distances is rather long at 2.83 Å. B atom B4 both chelates to Eu(1) and bridges to Eu(1)′ but does so unsymmetrically: the Eu(1)···B(4) distance is 3.215(6) Å, whereas the Eu(1)′···B(4) distance is 2.975(4) Å. The refined least-squares positions for the H atoms attached to B(4) suggest that only one H atom bridges to each of the metals, as shown in Figure 2. The Eu−O distances to the coordinated THF molecules are 2.582(2) and 2.605(2) Å, which closely match the Eu−O distances of 2.591(4) to 2.635(5) Å reported for $Eu(H_2BC_8H_{14})_2(THF)_4$. The Eu(1)−Eu(1)′ distance of 4.741(4) Å is far too long to suggest any metal−metal bonding.

We note in passing that the Eu atoms and the bridging DMADB ligands in **1** are each disordered over two sites in the solid state. The two sites are related by a pseudo-2-fold axis that runs the length of the molecule and passes approximately through the N atoms of the two terminal aminodiboranate ligands (Figure 3). The occupancy factor for the major site refined to 69%. The disorder adds to the uncertainty in the H atom locations, which are already uncertain owing to their small scattering factors.

Unlike **1**, the Yb(THF) complex **2** is monomeric (Figure 4); this structural difference is certainly attributable to the larger ionic radius of Eu^{II} (r_{ionic} = 1.17 Å) vs Yb^{II} (1.02 Å).[60] The arrangement of the B and O atoms in **2** is best described as a distorted cis octahedron because there are exactly three large interligand angles: B1−Yb1−B3 = 163.4(2)°, O2−Yb1−B4 = 140.5(2)°, and O1−Yb1−B2 = 134.2(1) (Table 3). The Yb···B distances range from 2.809(5) to 2.856(5) Å, and the Yb−O distances to the coordinated THF molecules are 2.397(3) and 2.416(3) Å. These distances are slightly shorter than those observed for $Yb(H_2BC_8H_{14})_2(THF)_4$, which are 2.876(7) Å (Yb···B) and 2.424(11) and 2.462(6) Å (Yb−O).[51] All of the BH_3 groups are bound to the Yb center by means of two hydrogen bridges; as expected, the κ^2H Yb−B distances in **2** are much longer than those observed for κ^3H tetrahydroborate groups bound to Yb^{II}, which range from 2.596(5) to 2.692(4) Å.[53,54] The Yb−H distances range from 2.35(3) to 2.54(3) Å and are consistent with those previously observed.[52−54]

The Eu(DME) complex **3** is monomeric; both DMADB ligands and both DME molecules chelate to the metal center (Figure 5). The four B atoms and the four O atoms describe a distorted square antiprism, in which the O atoms occupy one square face and the B atoms occupy the other. The Eu···B distances of 3.040(4)−3.115(4) Å are similar to those observed in the THF complex **1** (Table 4). In contrast, the four Eu−O distances of 2.579(2)−2.701(2) Å are longer than those observed in **1**, which suggests that **3** is sterically crowded. The H atoms in BH_3 were located in the difference maps and could be refined with light constraints; all of the BH_3 groups are bound to metal in a κ^2H fashion, with Eu−H distances that range from 2.55(3) to 2.77(3) Å. The steric crowding in **3** is reflected in the Eu···B, Eu−O, and Eu−H distances, which are all significantly longer than those in $Eu(H_2BC_8H_{14})_2(THF)_4$.[51]

Crystals of the Yb(DME) complex **4** suitable for diffraction studies could not be obtained.

NMR, IR, and Field Ionization (FI) Mass Spectra. Complexes **1** and **3** contain the highly paramagnetic f^7 Eu^{II} ion and are NMR-silent. In contrast, complexes **2** and **4** contain the diamagnetic f^{14} Yb^{II} ion and their ^1H and ^{11}B NMR resonances are readily observable. The ^1H NMR spectrum of **2** contains singlets at δ 2.45 for the NMe_2 protons and at δ 3.61 and 1.30 for the α and β THF protons, respectively. A broad 1:1:1:1 quartet at δ 2.63 is

(60) Shannon, R. D. *Acta Crystallogr., Sect. A* **1976**, *A32*, 751–767.

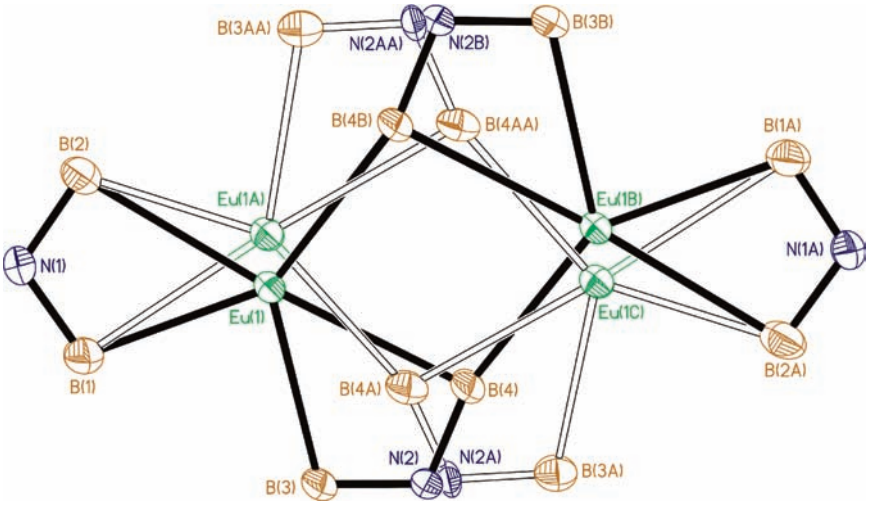

Figure 3. Single-crystal X-ray diffraction disorder model for **1**. Ellipsoids are drawn at the 35% probability level. Methyl groups, THF molecules, and H atoms have been removed for clarity.

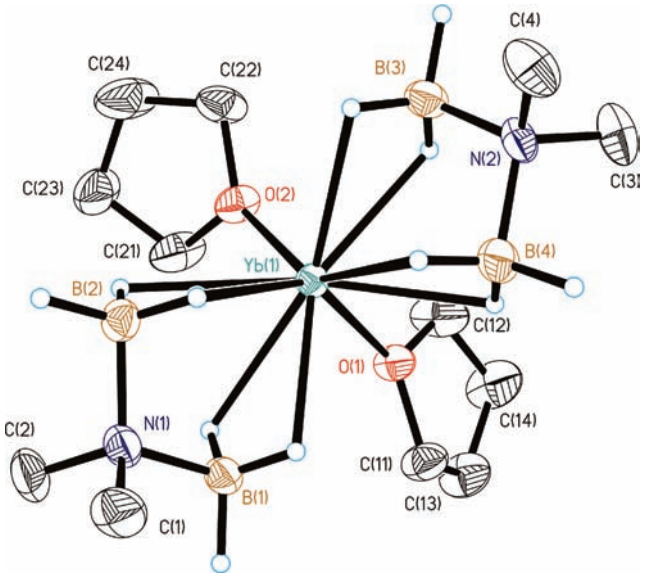

Figure 4. Molecular structure of **2**. Ellipsoids are drawn at the 35% probability level. H atoms attached to C atoms have been deleted for clarity.

assignable to the BH_3 group; the coupling constant to the ^{11}B nucleus ($I = {}^3/_2$) is 86 Hz. Evidently, exchange of the terminal and briding B−H groups within each BH_3 unit is rapid on the NMR time scale, as is observed for most metal-bound borohydride species.[61] The ^{11}B NMR spectrum of **2** consists of a 1:3:3:1 quartet at δ −7.7 due to coupling of the ^{11}B spin to the three H atoms.

The ^1H and ^{11}B NMR spectra of **4** are also readily observable. The ^1H NMR spectrum contains a singlet for the NMe_2 group at δ 2.50, a broad quartet for the BH_3 groups at δ 2.76, and DME resonances at δ 2.88 (CH_2) and 2.98 (OMe). Integration of the ^1H NMR resonances confirms the stochiometry determined from the microanalytical data. The ^{11}B NMR spectrum consists of a 1:3:3:1 quartet at δ −7.6.

Table 3. Selected Bond Lengths and Angles for **2**

Bond Lengths (Å)			
Yb(1)−O(2)	2.397(3)	Yb(1)−H(12)	2.35(3)
Yb(1)−O(1)	2.416(3)	Yb(1)−H(21)	2.43(3)
Yb(1)−B(1)	2.809(5)	Yb(1)−H(22)	2.53(3)
Yb(1)−B(3)	2.809(5)	Yb(1)−H(31)	2.44(4)
Yb(1)−B(2)	2.849(5)	Yb(1)−H(32)	2.43(4)
Yb(1)−B(4)	2.856(5)	Yb(1)−H(41)	2.54(3)
Yb(1)−H(11)	2.53(3)	Yb(1)−H(42)	2.45(4)
Bond Angles (deg)			
O(1)−Yb(1)−B(1)	81.98(13)	B(1)−Yb(1)−B(2)	55.34(15)
O(1)−Yb(1)−B(2)	134.17(13)	B(1)−Yb(1)−B(3)	163.39(16)
O(1)−Yb(1)−B(3)	104.25(14)	B(1)−Yb(1)−B(4)	109.65(17)
O(1)−Yb(1)−B(4)	95.20(16)	B(2)−Yb(1)−B(3)	121.43(16)
O(2)−Yb(1)−O(1)	81.40(12)	B(2)−Yb(1)−B(4)	113.03(18)
O(2)−Yb(1)−B(1)	108.78(14)	B(3)−Yb(1)−B(4)	54.96(17)
O(2)−Yb(1)−B(2)	96.09(14)	B(1)−N(1)−B(2)	111.1(4)
O(2)−Yb(1)−B(3)	87.52(14)	B(4)−N(2)−B(3)	111.1(3)
O(2)−Yb(1)−B(4)	140.50(15)		

The IR spectra of the THF complexes **1** and **2** both exhibit characteristic peaks between 2500 and 2000 cm^{-1} due to B−H stretches, but the two spectra are very different. The spectrum of **1** has two strong, broad peaks at 2299 and 2249 cm^{-1}, whereas that of **2** has four strong, well-defined peaks at 2357, 2303, 2271, and 2227 cm^{-1}. The high-energy peak at 2357 cm^{-1} seen for **2** is assigned to a terminal B−H stretch, whereas the lower energy peaks correspond to bridging B−H−M stretches. The B−H peaks are broader in the spectrum of **1**, probably as a result of the greater variety of bonding modes compared with **2**, as seen in the solid-state structure. The frequencies of the symmetric and asymmetric O−C−O stretches of the coordinated THF molecule, 880 and 1016 cm^{-1} for **1** and 879 and 1019 cm^{-1} for **2**, are similar to those previously reported.[62]

The IR spectra of **1**−**4** suggest that the metal−DMADB interaction is stronger in the Yb complexes than in the Eu complexes, possibly because the smaller Yb

(61) Eaton, G. R.; Lipscomb, W. N. *N.M.R. Studies of Boron Hydrides and Related Compounds*; Benjamin: New York, 1969; p 617.

(62) Clark, R. J. H.; Lewis, J.; Machin, D. J.; Nyholm, R. S. *J. Chem. Soc.* **1963**, 379–387.

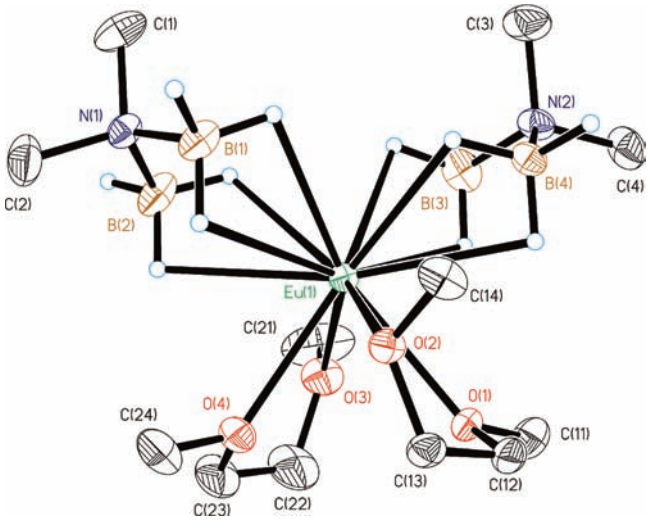

Figure 5. Molecular structure of **3**. Ellipsoids are drawn at the 35% probability level. H atoms attached to C atoms have been deleted for clarity.

Table 4. Selected Bond Lengths and Angles for **3**

Bond Lengths (Å)			
Eu(1)−O(3)	2.5786(19)	Eu(1)−H(11)	2.70(3)
Eu(1)−O(2)	2.6089(16)	Eu(1)−H(12)	2.65(3)
Eu(1)−O(4)	2.6705(18)	Eu(1)−H(21)	2.58(3)
Eu(1)−O(1)	2.7008(16)	Eu(1)−H(22)	2.75(3)
Eu(1)−B(3)	3.040(4)	Eu(1)−H(31)	2.55(3)
Eu(1)−B(1)	3.070(3)	Eu(1)−H(32)	2.60(3)
Eu(1)−B(4)	3.109(3)	Eu(1)−H(41)	2.57(2)
Eu(1)−B(2)	3.115(3)	Eu(1)−H(42)	2.77(3)
Bond Angles (deg)			
O(2)−Eu(1)−O(1)	63.70(5)	O(3)−Eu(1)−B(2)	83.74(8)
O(3)−Eu(1)−O(1)	71.07(6)	O(3)−Eu(1)−B(3)	84.03(9)
O(4)−Eu(1)−O(1)	73.92(6)	O(3)−Eu(1)−B(4)	125.06(8)
O(3)−Eu(1)−O(2)	124.34(6)	O(4)−Eu(1)−B(1)	94.49(8)
O(2)−Eu(1)−O(4)	74.17(5)	O(4)−Eu(1)−B(2)	82.42(9)
O(3)−Eu(1)−O(4)	63.23(7)	O(4)−Eu(1)−B(3)	147.12(8)
O(1)−Eu(1)−B(1)	146.78(7)	O(4)−Eu(1)−B(4)	150.19(7)
O(1)−Eu(1)−B(2)	151.15(8)	B(1)−Eu(1)−B(2)	49.77(8)
O(1)−Eu(1)−B(3)	93.54(9)	B(3)−Eu(1)−B(1)	110.72(11)
O(1)−Eu(1)−B(4)	82.15(7)	B(1)−Eu(1)−B(4)	96.00(9)
O(2)−Eu(1)−B(1)	83.29(7)	B(3)−Eu(1)−B(2)	97.68(12)
O(2)−Eu(1)−B(2)	125.34(8)	B(4)−Eu(1)−B(2)	125.02(10)
O(2)−Eu(1)−B(3)	127.87(8)	B(3)−Eu(1)−B(4)	50.08(9)
O(2)−Eu(1)−B(4)	79.45(7)	B(1)−N(1)−B(2)	110.6(2)
O(3)−Eu(1)−B(1)	131.81(8)	B(4)−N(2)−B(3)	110.5(2)

ion is more strongly Lewis acidic. Specifically, the energy differences between the principal terminal and bridging B−H stretches are 50 and 47 cm^{-1} in **1** and **3** versus 130 and 98 cm^{-1} for **2** and **4**.

For the DME complexes, the IR spectrum of the Eu compound **3** contains strong, well-resolved terminal and bridging B−H stretches at 2302 and 2255 cm^{-1}, respectively, whereas the IR spectrum of the Yb compound **4** has three strong peaks at 2331, 2296, and 2233 cm^{-1}. Two peaks at 852 and 1006 cm^{-1} in **3** and two at 861 and 1105 cm^{-1} in **4** correspond to the C−O−C stretches of the coordinated DME molecules.

The Eu compound **1** gives no metal-containing species in its FI mass spectrum, but the spectrum of **2** contains envelopes of metal-containing ions centered at values of m/z 317, 388, and 704. The assignment of formulas to these ions is somewhat complicated by the similar molecular weights of THF (72.11 g mol^{-1}) and the DMADB ligand (71.75 g mol^{-1}). Analysis of the isotropic distributions suggests that the peaks in the mass spectrum are best assigned as follows: the m/z 317 envelope is a mixture of $Yb(H_3BNMe_2BH_3)(THF)^+$ and $Yb(H_3BNMe_2BH_3)_2^+$, the m/z 388 envelope is a mixture of $Yb(H_3BNMe_2BH_3)(THF)_2^+$ and $Yb(H_3BNMe_2BH_3)_2(THF)^+$, and the envelope at m/z 704 is a mixture of $Yb_2(H_3BNMe_2BH_3)_3(THF)_2^+$ and $Yb_2(H_3BNMe_2BH_3)_4(THF)^+$.

Compound **3** does not give metal-containing ions in its FI mass spectrum, but **4** gives a strong parent peak at m/z 406 corresponding to $Yb(H_3BNMe_2BH_3)_2(DME)^+$.

Concluding Remarks. Like BH_4^-, the aminodiboranate anion $H_3BNMe_2BH_3^-$ is able to serve both as a ligand and as a reductant for lanthanides, but only the two most easily reduced lanthanides, Eu and Yb, are converted from the 3+ to 2+ oxidation state. In the analogous reaction of $SmCl_3$ with $Na(H_3BNMe_2BH_3)$, there is no evidence of a reduction to Sm^{II}. As discussed above, for both Eu and Yb, a mixture of the lanthanide(II) and lanthanide(III) aminodiboranate products is generated, with the ratio being temperature-dependent: the Ln^{II} products are favored if the metal trichloride is mixed with $Na(H_3BNMe_2BH_3)$ at higher temperatures. Relevant in the current context is our finding that $Na(H_3BNMe_2BH_3)$ is able to reduce U^{IV} to U^{III}.[58]

The aqueous Ln^{3+}/Ln^{2+} reduction potentials of these metals are Eu (−0.36 V), Yb (−1.05 V), and Sm (−1.55 V), and the redox potential of the U^{4+}/U^{3+} couple is −0.61 V.[63] The reduction chemistry that we see with the aminodiboranate anion cannot be under thermodynamic control: the anion cannot be simultaneously a strong enough reductant to reduce U^{IV} to U^{III} and also too weak to convert Eu^{III} completely to Eu^{II}. Instead, kinetic steps involving the breaking of B−H bonds and the reductive elimination of H_2 are almost certainly involved in the reduction chemistry (as they are for BH_4^-),[64] and the barriers associated with these steps are evidently metal-dependent.

Experimental Section

All operations were carried out in a vacuum or under argon using standard Schlenk techniques. All glassware was dried in an oven at 150 °C, assembled hot, and allowed to cool under a vacuum before use. Tetrahydrofuran (THF), 1,2-dimethoxyethane (DME), diethyl ether, and pentane were distilled under nitrogen from sodium/benzophenone and degassed with argon immediately before use. Anhydrous $LnCl_3$ (Strem) and LnI_2 (Aldrich) were used as received. $Na(H_3BNMe_2BH_3)$ was prepared by a literature route.[57]

Elemental analyses were carried out by the University of Illinois Microanalytical Laboratory. The IR spectra were recorded on a Nicolet Impact 410 infrared spectrometer as Nujol mulls between KBr plates. The ^1H NMR data were obtained on a Varian Unity 400 instrument at 400 MHz or on a Varian Unity U500 instrument at 500 MHz. The ^{11}B NMR

(63) Lide, D. R. *CRC Handbook of Chemistry and Physics*, 77th ed.; CRC Press: Boca Raton, 1996; p 2512.
(64) Glavee, G. N.; Klabunde, K. J.; Sorensen, C. M.; Hadjipanayis, G. C. *Langmuir* **1994**, *10*, 4726–4730.

data were collected on a General Electric GN300WB instrument at 96 MHz or on a Varian Unity Inova 600 instrument at 192 MHz. Chemical shifts are reported in δ units (positive shifts to high frequency) relative to tetramethylsilane (^{1}H NMR) or $BF_3 \cdot Et_2O$ (^{11}B NMR). FI mass spectra were recorded on a Micromass 70-VSE mass spectrometer. The shapes of all peak envelopes correspond with those calculated from the natural abundance isotopic distributions in the observed spectra. Melting points and decomposition temperatures were determined in closed capillaries under argon on a Thomas-Hoover Unimelt apparatus.

Caution! *Complexes* ***2*** *and* ***4*** *enflame upon exposure to air.*

Bis[*N*,*N*-dimethylaminodiboranato]bis(tetrahydrofuran)europium(II), Eu($H_3BNMe_2BH_3$)$_2$(THF)$_2$ (1). Method A. To a suspension of $EuCl_3$ (0.50 g, 1.9 mmol) in THF (20 mL) at 0 °C was added a solution of sodium *N*,*N*-dimethylaminodiboranate (0.56 g, 5.9 mmol) in THF (20 mL). The gray reaction mixture was stirred at 0 °C for 15 min and then was warmed to room temperature. The solution over the gray suspension slowly became yellow. The mixture was stirred for 40 h at room temperature and then was evaporated to dryness under a vacuum to afford a sticky yellow solid. The residue was extracted with pentane (2 × 20 mL). The pale-yellow extracts were filtered, combined, concentrated to ca. 15 mL, and cooled to −20 °C to yield off-white crystals. Yield: 0.39 g (47%). Anal. Calcd for $C_{12}H_{40}B_4N_2O_2Eu$: C, 32.8; H, 9.17; N, 6.37. Found: C, 31.5; H, 9.04; N, 6.41. Although the first crop was pure **1**, subsequent crops contained increasing amounts of the intensely yellow trivalent complex Eu($H_3BNMe_2BH_3$)$_3$(THF).[65]

Method B. To a suspension of EuI_2 (0.52 g, 1.3 mmol) in THF (20 mL) was added a solution of sodium *N*,*N*-dimethylaminodiboranate (0.25 g, 2.6 mmol) in THF (20 mL). Most of the EuI_2 suspension immediately dissolved, and the yellow mixture was stirred for 20 h and then evaporated to dryness under a vacuum to afford a sticky light-yellow solid. The residue was extracted with pentane (55 mL), and the pale-yellow extract was filtered, concentrated to 20 mL, and cooled to −20 °C to yield 0.26 g of pale-yellow crystals. Concentrating the mother liquor to 5 mL and cooling it to −20 °C yielded an additional 0.04 g of crystals. Yield: 0.30 g (53%). Mp: 74−76 °C. Anal. Calcd for $C_{12}H_{40}B_4N_2O_2Eu$: C, 32.8; H, 9.17; N, 6.37. Found: C, 32.2; H, 9.31; N, 6.50. IR (cm^{-1}): 2397 w, 2321 sh, 2299 vs, 2249 vs, 2068 w, 1339 w, 1247 m, 1227 m, 1208 m, 1177 s, 1153 s, 1143 s, 1038 s, 1016 s, 967 w, 927 m, 902 m, 880 s, 797 w.

Bis[*N*,*N*-dimethylaminodiboranato]bis(tetrahydrofuran)ytterbium(II), Yb($H_3BNMe_2BH_3$)$_2$(THF)$_2$ (2). Method A. To a suspension of $YbCl_3$ (0.55 g, 2.0 mmol) in THF (15 mL) was added a solution of sodium *N*,*N*-dimethylaminodiboranate (0.56 g, 5.9 mmol) in THF (15 mL). The off-white reaction mixture was stirred for 15 h at room temperature and then evaporated to dryness under a vacuum to afford a sticky yellow residue. The residue was extracted with pentane (50 mL), and the intense yellow extract was filtered, concentrated to ca. 15 mL, and cooled to −20 °C to yield intense-yellow crystals. Yield: 0.35 g (39%). Anal. Calcd for $C_{12}H_{40}B_4N_2O_2Yb$: C, 31.3; H, 8.75; N, 6.08. Found: C, 30.7; H, 9.04; N, 6.41. NMR data match those of **2** obtained by method B. Although the first crop was pure **2**, subsequent crops contained increasing amounts of the pale-yellow trivalent complex Yb($H_3BNMe_2BH_3$)$_3$(THF). This compound can be readily distinguished by its NMR spectra, which reflect the paramagnetism of the Yb^{III} ion.[65]

Method B. To a suspension of YbI_2 (0.50 g, 1.2 mmol) in THF (20 mL) was added a solution of sodium *N*,*N*-dimethylaminodiboranate (0.22 g, 2.3 mmol) in THF (20 mL). Most of the YbI_2 suspension slowly dissolved, and the yellow mixture was stirred for 24 h and then evaporated to dryness under a vacuum to afford a sticky intense-yellow solid. The residue was extracted with pentane (40 mL), and the intense-yellow extract was filtered, concentrated to 22 mL, and cooled to −20 °C to yield 0.37 g of pale-yellow crystals. Concentrating the mother liquor to 8 mL and cooling it to −20 °C yielded an additional 0.03 g of crystals. Yield: 0.40 g (74%). Mp: 110−113 °C. Anal. Calcd for $C_{12}H_{40}B_4N_2O_2Yb$: C, 31.3; H, 8.75; N, 6.08. Found: C, 30.5; H, 8.81; N, 6.08. ^{1}H NMR (C_7D_8, 20 °C): δ 1.30 (s, fwhm = 20 Hz, β-CH_2, 8 H), 2.45 (s, fwhm = 12 Hz, NMe_2, 12 H), 2.63 (br q, J_{BH} = 86 Hz, BH_3, 12 H), 3.61 (s, fwhm = 20 Hz, α-CH_2, 8 H). ^{11}B NMR (C_7D_8, 20 °C): δ −7.7 (q, J_{BH} = 91 Hz, BH_3). MS(FI) [fragment ion, relative abundance]: *m*/*z* 115 [H_2BNMe_2-BH_2NMe_2, 60], 316 [Yb($H_3BNMe_2BH_3$)$_2$, 60], 376 [Yb(H_3B-NMe_2BH_3)$_3$−BH_2, 45], 388 [Yb($H_3BNMe_2BH_3$)$_2$(THF)/Yb($H_3BNMe_2BH_3$)(THF)$_2$, 100], 704 [Yb$_2$($H_3BNMe_2BH_3$)$_4$-(THF)/Yb$_2$($H_3BNMe_2BH_3$)$_3$(THF)$_2$, 55]. IR (cm^{-1}): 2385 sh, 2357 vs, 2303 m, 2271 s, 2227 vs, 2075 w, 1342 w, 1261 m, 1232 m, 1211 m, 1177 s, 1147 s, 1031 s, 1019 s, 931 m, 918 w, 905 m, 879 m, 801 m.

Bis[*N*,*N*-dimethylaminodiboranato]bis(1,2-dimethoxyethane)europium(II), Eu($H_3BNMe_2BH_3$)$_2$(DME)$_2$ (3). To a suspension of **1** (0.22 g, 0.50 mmol) in pentane (16 mL) was added DME (0.5 mL, 5 mmol). A thick gray precipitate formed immediately. The mixture was stirred for 2 h and then was filtered. The filtrate was discarded, and the solid was washed with pentane (10 mL) and dried under a vacuum to yield a light-gray powder. Yield: 0.17 g (71%). The concentration and cooling of solutions of **3** in diethyl ether produced large, cubic crystals suitable for diffraction studies. Mp: 107−115 °C (dec). Anal. Calcd for C_{12}-$H_{44}B_4N_2O_4Eu$: C, 30.3; H, 9.32; N, 5.89. Found: C, 29.8; H, 9.32; N, 5.87. IR (cm^{-1}): 2391 w, 2366 w, 2347 sh, 2302 vs, 2255 s, 2226 sh, 2071 w, 1303 w, 1254 w, 1223 m, 1210 m, 1178 s, 1152 s, 1106 m, 1060 s, 1016 s, 979 w, 926 m, 904 w, 852 s, 802 w.

Bis[*N*,*N*-dimethylaminodiboranato](1,2-dimethoxyethane)ytterbium(II), Yb($H_3BNMe_2BH_3$)$_2$(DME) (4). To a bright-yellow suspension of **2** (0.22 g, 0.48 mmol) in pentane (16 mL) was added DME (0.5 mL, 5 mmol). Most of the solid dissolved immediately. The mixture was stirred for 2 h, and the intense-yellow mixture was filtered, concentrated to 3 mL, and cooled to −20 °C to yield an intense-yellow semicrystalline solid. Yield: 0.16 g (82%). Mp: 107−115 °C (dec). Anal. Calcd for $C_8H_{34}B_4N_2O_2Yb$: C, 23.6; H, 8.43; N, 6.89. Found: C, 23.9; H, 8.69; N, 6.73. ^{1}H NMR (C_6D_6, 20 °C): δ 2.50 (s, fwhm = 15 Hz, NMe_2, 12 H), 2.76 (br q, J_{BH} = 90 Hz, BH_3, 12 H), 2.88 (s, fwhm = 16 Hz, CH_2, 4 H), 2.98 (s, fwhm = 20 Hz, CH_3, 6 H). ^{11}B NMR (C_7D_8, 20 °C): δ −7.6 (q, J_{BH} = 91 Hz, BH_3). MS(FI) [fragment ion, relative abundance]: *m*/*z* 115 [H_2BNMe_2-BH_2NMe_2, 100], 406 [Yb($H_3BNMe_2BH_3$)$_2$(DME), 25]. IR (cm^{-1}): 2391 w, 2331 vs, 2296 vs, 2233 vs, 2071 w, 1303 w, 1286 w, 1265 w, 1233 m, 1214 m, 1178 s, 1149 s, 1105 m, 1069 sh, 1060 s, 1020 s, 944 w, 929 m, 906 w, 861 m, 834 w, 805 w.

Crystallographic Studies.[66] Single crystals of **1** and **2**, grown from pentane, and **3**, grown from diethyl ether, were mounted on glass fibers with Paratone-N oil (Exxon) and immediately cooled to −80 °C in a cold-nitrogen gas stream on the diffractometer. Standard peak search and indexing procedures, followed by least-squares refinement, yielded the cell dimensions given in Table 1. Data were collected with an area detector by using the measurement parameters listed in Table 1. For all crystals, the measured intensities were reduced to structure factor amplitudes and their estimated standard deviations by correction for background and Lorentz and polarization effects. Although corrections for crystal decay were unnecessary, face-indexed absorption corrections were applied. Systematically absent reflections were deleted, and symmetry-equivalent reflections were averaged to yield a set of unique data. All unique data were used in the least-squares refinements.

(65) Daly, S. R.; Kim, D. Y.; Girolami, G. S., manuscript in preparation.

(66) Brumaghim, J. L.; Priepot, J. G.; Girolami, G. S. *Organometallics* **1999**, *18*, 2139–2144.

The structures were solved using direct methods (*SHELXTL*). The correct position of all of the non-H atoms were deduced from *E* maps and subsequent difference Fourier calculations. The analytical approximations to the scattering factors were used, and all structure factors were corrected for both real and imaginary components of anomalous dispersion. Unless otherwise stated, the refinement models had the following features: (1) Independent anisotropic displacement factors were refined for the non-H atoms. (2) Methylene and methyl H atoms were placed in idealized positions with C−H = 0.99 and 0.98 Å, respectively. (3) The methyl groups were allowed to rotate about the C−N bonds to find the best least-squares positions. (4) Methylene and methyl H atoms were given displacement parameters equal to 1.2 and 1.5 times U_{eq} for the attached C atom, respectively. In **1**, the boranyl H atoms were placed in idealized positions with B−H = 1.15 Å and were given displacement parameters equal to 1.2 times U_{eq} for the attached B atom, and the boranyl groups were allowed to rotate about the B−N bonds to find the best least-squares positions. The H atoms attached to B atoms in **2** and **3** were located in the difference maps, and their positions were refined with independent isotropic displacement parameters. No corrections for isotropic extinction were necessary. For all data sets, successful convergence was indicated by the maximum shift/error of 0.000 for the last cycle. Unless otherwise stated, a final analysis of the variance between observed and calculated structure factors showed no apparent errors. Final refinement parameters are given in Table 1. Aspects specific to the individual refinements are detailed in the following paragraphs.

Compound 1. The monoclinic lattice and systematic absences $0k0$ ($k \neq 2n$) and $h0l$ ($l \neq 2n$) were uniquely consistent with the space group $P2_1/c$, which was confirmed by the success of the subsequent refinement. The Eu centers and the bridging aminodiboranate ligands are disordered over two positions related by a pseudo-2-fold axis running along the length of the molecule and passing approximately through the N atoms of the two terminal aminodiboranate ligands. The terminal aminodiboranate ligands and some of the atoms of the THF molecules of the two disordered components are essentially superimposed and could be refined as full-occupancy groups. The site occupancy factors (SOFs) for the disordered atoms were constrained to sum to 1; the SOF for the major occupancy component refined to 0.690. The THF molecules show further disorder; only the α-C atoms are disordered in one molecule, whereas all of the C atoms are disordered in the other. The SOFs for the disordered components were also constrained to sum to 1; the SOF for the major occupancy components refined to 0.512 and 0.563, respectively. The quantity minimized by the least-squares program was $\sum w(F_o^2 - F_c^2)^2$, where $w = \{[\sigma(F_o)]^2 + (0.421P)^2\}^{-1}$ and $P = (F_o^2 + 2F_c^2)/3$. The chemically equivalent C−N, B−N, B···C, and C···C distances within the aminodiboranate ligands were constrained to be equal within an esd of 0.005 Å. The C−O and C−C distances in the THF molecules were constrained to be 1.48 ± 0.005 and 1.52 ± 0.005 Å, respectively. The largest peak in the final Fourier difference map (0.65 e Å^{-3}) was located 0.95 Å from Eu1.

Compound 2. The monoclinic lattice and systematic absences $0k0$ ($k \neq 2n$) and $h0l$ ($h + l \neq 2n$) were uniquely consistent with the space group $P2_1/n$, which was confirmed by the success of the subsequent refinement. The quantity minimized by the least-squares program was $\sum w(F_o^2 - F_c^2)^2$, where $w = \{[\sigma(F_o)]^2 + (0.0578P)^2\}^{-1}$ and $P = (F_o^2 + 2F_c^2)/3$. The chemically equivalent B−H and H···H distances were constrained to be equal within 0.01 Å. The largest peak in the final Fourier difference map (2.65 e Å^{-3}) was located 0.82 Å from Yb1.

Compound 3. The monoclinic lattice and systematic absences $0k0$ ($k \neq 2n$) and $h0l$ ($h + l \neq 2n$) were uniquely consistent with the space group $P2_1/n$, and this choice was confirmed by successful refinement of the proposed model. The quantity minimized by the least-squares program was $\sum w(F_o^2 - F_c^2)^2$, where $w = \{[\sigma(F_o)]^2 + (0.0210P)^2\}^{-1}$ and $P = (F_o^2 + 2F_c^2)/3$. The chemically equivalent B−H distances were constrained to be equal within an esd of 0.01 Å. The largest peak in the final Fourier difference map (0.83 e Å^{-3}) was located 1.03 Å from C22.

Acknowledgment. We thank the National Science Foundation (Grants CHE07-50422 and DMR-0420768) and the PG Research Foundation for support of this research and Scott Wilson, Teresa Wieckowska-Prussak, and Danielle Gray for collecting the X-ray diffraction data. We also thank Brian Bellott for taking photographs of the crystal mixtures of **1** and $Eu(H_3BNMe_2BH_3)_3(THF)$.

Supporting Information Available: X-ray crystallographic data in CIF format. This material is available free of charge via the Internet at http://pubs.acs.org.